Amorphous Complexes $MM(EDTA)(H_2O)_4 \cdot 2H_2O$. LAXS and XPS Investigation of the Local Structure

Ruggero Caminiti

Dipartimento di Chimica-Università di Roma- "La Sapienza" Roma, Italy

Carmen Munoz Roca, Daniel Beltran-Porter

Department de Quimica Inorganica-Universidad de Valencia, Valencia, Spain

Antonella Rossi

Istituto di Chimica Generale, Inorganica ed Analitica, Università di Cagliari, Cagliari, Italy

Z. Naturforsch. **43a**, 591–596 (1988); received February 3, 1988

The amorphous $MM(EDTA)(H_2O)_4 \cdot 2H_2O$ (M = Ni, Co) substances are made up of infinite chains of alternating "hydrated" and "chelated" octahedra bridged by carboxylate groups: $M(H_2O)_4 - M(EDTA) - M(H_2O)_4 - \ldots$.

XPS enables to ascertain that the coordination of the EDTA ligand in the amorphous phase is identical to that in the crystalline phase, i.e., hexacoordination toward the M atom and two bridging groups in the Ni–Ni, Co–Co compounds.

Introduction

The Large-Angle X-ray Scattering (LAXS) is a very useful tool for investigating short range order in liquid and amorphous systems [1–4].

The ESCA technique has proved to be very convenient for studying transition metal complexes since its first discovery [5–6] and has been applied to the investigation of many Ni- and Co-compounds.

The most extensive studies of nickel compounds by ESCA are due to Matienzo et al. [7] and Tolman et al. [8].

Matienzo et al. [7] studied the XPS spectra of Ni2p3/2 levels for about 70 compounds containing nickel in all of its known oxidation states. The binding energies have been correlated with ligand electronegativities, delocalization of charge on the ligands and stereochemistry; the shake-up satellites were studied to establish a relationship between the shake-up transition and paramagnetism. Tolman et al. [8] reported the XPS data for all of the elements in 46 nickel compounds containing a variety of ligands and with formal oxidation states of 0, +2, and +4 including olefin, alkyl, aryl, and -allyl organometallic complexes.

Reprint requests to Prof. R. Caminiti, Dipartimento di Chimica, Università di Roma, "La Sapienza", P. le Aldo Moro 7, 00184 Roma (Italy).

These investigations demonstrated the possibility of distinguishing between square-planar and octahedral complexes since the diamagnetic square-planar complexes do not exhibit satellite structure.

Cobalt complexes have also been investigated by means of XPS [9–10]: thus it is possible to distinguish between cobalt(II) (d^7, high spin, 4F) and cobalt(II) (d^7, low spin, 2D); the satellites are much more pronounced in high spin than in low spin systems.

In this paper we present the results of our studies by means LAXS and XPS on amorphous and crystalline $CO_2(EDTA) \cdot 6H_2O$ and $Ni_2(EDTA) \cdot 6H_2O$ complexes. Both complexes belong to a series formulated as $MM(EDTA)(H_2O)_4 \cdot 2H_2O$ [11–13]. The structural organization consists of infinite zigzag chains of polymer-like compounds $[MM(EDTA)(H_2O)_4]$ with Co(1) or Ni(1) atom coordinated by the two nitrogen atoms and four oxygen atoms of an $EDTA^{4-}$ ion, whereas the second metallic atom (Co(2) or Ni(2)) is coordinated by two oxygen atoms of the $EDTA^{4-}$ ion and four water molecules.

Experimental

Preparation of the Complexes

An aqueous solution of $Na_4(EDTA) \cdot 2H_2O$ was mixed with stoichiometric quantities of the corre-

0932-0784 / 88 / 0600-0591 $ 01.30/0. – Please order a reprint rather than making your own copy.

sponding nitrates of Co and Ni dissolved in water. After filtration of the resulting solution, excess of aceton was added with stirring and a slimy solid was obtained. This solid, separated by decantation and dried in air, appears as blue (Ni_2 complex) or purple (Co_2 complex) pellets. These compounds were characterized by means of the traditional techniques.

X-Ray Scattering Measurements and Data Treatment

The samples were very finely ground, introduced into a vessel and pressed at about 9 kg/cm^2. The volume of the vessel was about 13 cm^3.

The spectrum scattered by the sample irradiated with molybdenum kα radiation ($\lambda = 0.7107$ Å) was obtained by using an θ-θ automatic diffractometer. The measured intensity was recorded in the s range from 0.6 to 15.5 Å^{-1}, where $s = (4\pi/\lambda)\sin\theta$. About 100 000 counts were collected for each point, and each angular region was scanned twice. The applied correction and normalization process adopted was the same as in [14]. Atomic scattering factors, $f_i(s)$ for all the atoms were taken from Int. Tables [15]. Compton diffusion factors were taken from tables published by Cromer [16]. Reduced intensities were calculated with the equation

$$i(s) = K I_c(s) - \sum_i n_i [(f_i(s) + \Delta f_i')^2 + \Delta f_i'' + I_{i\,(\mathrm{inch})}(s) \cdot \mathrm{del}(s)], \quad (1)$$

where K is the normalization constant, $I_c(s)$ the corrected intensity, n_i the number of atoms i in the chosen unit volume, $f_i(s)$ the atomic scattering factor, $\Delta f_i'$ and $\Delta f_i''$ are the real and imaginary part of the anomalous dispersion, $I_{i\,(\mathrm{inch})}(s)$ is the total incoherent radiation for the atom i and del(s) the fraction of the total incoherent scattering reaching the counter. si(s) vs. s is shown in Fig. 1 for the two samples.

The radial distribution $D(r)$ is then expressed by

$$D(r) = 4\pi r^2 \varrho_0 + 2r\pi^{-1} \int_0^{s_{\max}} s \cdot i(s)\, M(s) \sin(rs)\, \mathrm{d}s,$$

where ϱ_0 is the average electronic density of the sample, ($\varrho_0 = (\sum_i n_i f_i(0))^2 V^{-1}$), V is the stoichiometric unit volume chosen and $M(s)$ a modification function defined by

$$f_{Co}^2(0)/f_{Co}^2(s) \exp(-0.01\, s^2).$$

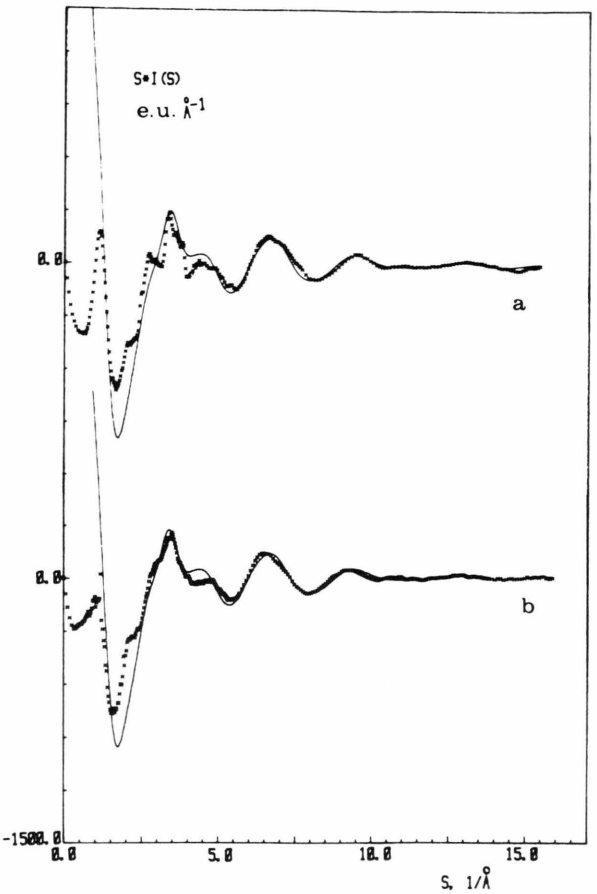

Fig. 1. Observed ($\times\times\times$) and calculated (——) si(s) values vs. $s = 4\pi\lambda^{-1}\sin\theta$ for the $Ni_2(EDTA)(H_2O)_4 \cdot 2H_2O$ (a) and $Co_2(EDTA)(H_2O)_4 \cdot 2H_2O$ (b) amorphous materials.

For the upper integration limit, $s_{\max}$, the same value, 15, 5 Å^{-1} was used for both samples.

In Fig. 2 the experimental radial distribution functions in the form Diff$(r) = D(r) - 4\pi r^2 \varrho_0$ for the two samples (Ni – Ni and Co – Co) are shown.

Theoretical peaks were calculated by a corresponding Fourier transformation of the theoretical intensities for the pair interactions,

$$i_{pq} = \sum f_p f_q \sin(r_{pq} s)(r_{pq} s)^{-1} \exp(-1/2\, \sigma_{pq}^2 s^2)$$

using the same sharpening function and the same $s_{\max}$ value as for the experimental data and assuming the rms variation in the distance to be σ_{pq}.

X-ray Photoelectron Spectroscopy Measurements

The instrument used in this investigation was an ESCALAB MK II induced electron emission spec-

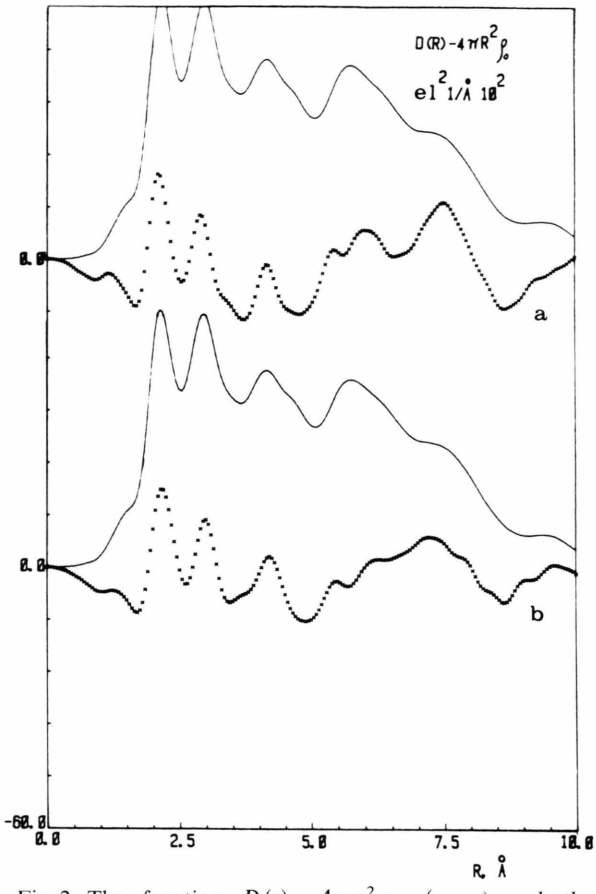

Fig. 2. The function $D(r) - 4\pi r^2 \varrho_0$ (× × ×) and the theoretical peak shapes (——) calculated as described in the paper, for the $Ni_2(EDTA)(H_2O)_4 \cdot 2H_2O$ (a) and $Co_2(EDTA)(H_2O)_4 \cdot 2H_2O$ (b) amorphous materials.

trometer with an Alk α X-ray source (1486.6 eV, 20 mA, 14 kV) manufactured by Vacuum Generator Ltd., East Grinstead, U.K.

The samples were mounted as pellets on a nickel sample holder and cooled with liquid nitrogen. The vacuum system of the instrument consisted of a nitrogen-trapped turbomolecular pump and a titanium sublimation pump for the analyser chamber.

The residual pressure in the spectrometer during the runs was about 10^{-7} Pa. All the spectra were obtained in the digital mode using computer control of the measurements (Apple IIe P. C. with VGS 1000 Software). No radiation damage during the measurements was observed since the spectra were repeated several times. Cooling of the samples to liquid N_2 temperature was performed against possible secondary decomposition effects. Whenever possible the spectra were resolved into their Gaussian-Lorentian components. To compensate for sample charging during the analysis, all binding energies were referenced to the carbon 1 s signal at 285.0 eV due to external contamination. The accuracy of the measured binding energies was estimated as + 0.2 eV. For instrument calibration the Au 4f 7/2 line (83.8 eV) from a gold sheet was used.

Results and Discussion

Structural Analysis

The objective of this structural study was the comparison of the structural order around the metal (M) in these amorphous compounds with that present in the crystalline complexes [11–12]. $Ni_2(EDTA)(H_2O)_4 \cdot 2H_2O$ has been previously studied [2]. The structural model proposed by Mosset et al. [2] reproduces the LAXS data.

Our experimental structure function of $Ni_2(EDTA)(H_2O)_4 \cdot 2H_2O$ is very similar to that published in [2]. Only in the low angle region the height of the first peak at about 1 $Å^{-1}$ is different. This produces differences in the Diff. (r) function in the long-distances region. It should be noted that the sample described in [2] was much more pressed than that investigated in the present paper (3000 kg cm^{-2} vs. 9 kg cm^{-2}). Comparison of the CoCo and NiNi experimental structure functions reveals a difference in the height of the first peak, whereas the shape for $s > 1.5$ $Å^{-1}$ is very similar. A qualitative analysis of the Diff. (r) functions (NiNi and CoCo) shows the occurence of four well-defined peaks at about 1.25, 2.10, 2.95 and 4.15 Å.

Each of these peaks derives from numerous contributions of different origin: metal-light atom interactions and light-atom light-atom interactions. The "short" metal-metal distance is 5.58 Å in the NiNi and 5.58 Å in the CoCo crystal structure [12].

Comparison between experimental radial distribution functions of both NiNi and CoCo amorphous compounds (Fig. 2) leads to conclude that these complexes are characterized by nearly identical peaks centered on the same r values. The short range order suggested by these peaks is consistent with that existing in the crystalline structure of $Co_2(EDTA)(H_2O)_4 \cdot 2(H_2O)$ [12].

Synthetic structure functions were calculated; as in [1, 4, 14], the contribution from the discrete interactions is accounted for by using the Debye formula

modified so that a Gaussian-type distribution of interatomic distances can be introduced. The mean positions of atoms were assumed to be those reported by McCandlish et al. [12]; none of the inside unit distances were thus considered as indipendent parameters. The only independent parameters used were the mean square deviations of the interatomic distances. However, to each distance falling within a preset range (for example 1.0–1.7 Å, 1.7–2.5 Å, 2.5–3.5 Å and so on) the same value of mean square deviation was assigned, so that the number of adjusted parameters was much smaller than the number of pair distances existing in the model.

The calculation proved that the model is consistent with the experimental data. In order to compare Diff.(r) and theoretical peak shapes, a Fourier transformation of the theoretical structure functions was performed. In Fig. 2 the experimental Diff.(r) and theoretical peak shapes are shown.

The agreement between model and experiments was achieved without refining the interatomic distances which were taken from the crystalline model [12].

The final parameters of the adjusted parameters are quite reasonable; the mean square deviation tends to increase with interatomic distances.

The values are reported in Table 1. The consistency between model and experimental data is, of course, only a necessary condition for the model to be judged valid.

$1 < r \leq 1.7$ Å	$\sigma_1 = 0.06$
$1.7 < r \leq 2.5$ Å	$\sigma_2 = 0.12$
$2.5 < r \leq 3.5$ Å	$\sigma_3 = 0.14$
$3.5 < r \leq 5.0$ Å	$\sigma_4 = 0.18$
$5.0 < r \leq 6.0$ Å	$\sigma_5 = 0.25$
$6.0 < r \leq 20$ Å	$\sigma_6 = 0.30$

Table 1. The final values of the adjusted parameters ($rms\ \sigma_{pq}$) for the model used.

Table 2. Core-level binding energies of cations.

Compound	2p3/2 (eV)	2p1/2 (eV)	2p1/2 − 2p3/2 (eV)	FWHM (eV)
Ni	852.8	870.1	17.3	2.5
$Ni_2(EDTA)\cdot 6(H_2O)$ amorphous	855.0	872.4	17.4	2.9
$Ni_2(EDTA)\cdot 6(H_2O)$ crystalline	855.1	872.5	17.4	2.6
Co	778.5	793.5	15.1	2.5
$Co_2(EDTA)\cdot 6(H_2O)$ amorphous	781.0	796.6	15.6	3.9
$Co_2(EDTA)\cdot 6(H_2O)$ crystalline	780.8	796.4	15.6	3.7

X-Ray Photoelectron Data

Figure 3 shows the 2p levels of Ni in $Ni_2(EDTA)(H_2O)_4\cdot 2(H_2O)$, amorphous and crystalline. Table 2 gives the corresponding binding energy values (BE).

The binding energy of the Ni 2p levels and the spin-orbit splitting (17.4 eV) are in good agreement with literature data [7–8]. The 2p levels of the cation in $Ni_2(EDTA)(H_2O)_4\cdot 2(H_2O)$ are found to be shifted by 2.2 eV towards higher binding energy compared to the nickel metallic signal taken as reference.

There is no appreciable change in the 2p1/2–2p3/2 separation. The 2p region exhibits additional lines on the binding energy side of the main peaks.

The presence of satellite structure indicates that the compound is paramagnetic and, in agreement with LAXS analysis, has octahedral configuration. The same type of behaviour was observed for paramagne-

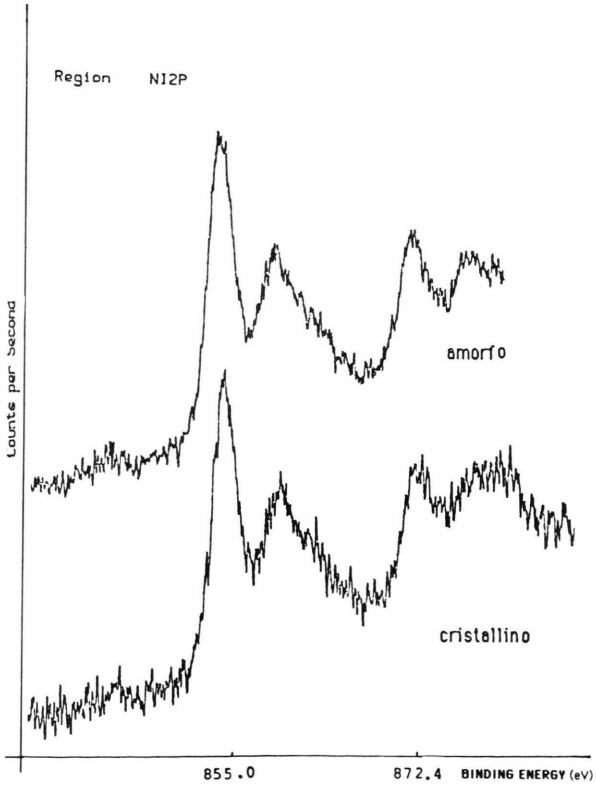

Fig. 3. XPS spectra of Ni2p levels for $Ni_2(EDTA)\cdot 6H_2O$, amorphous and crystalline.

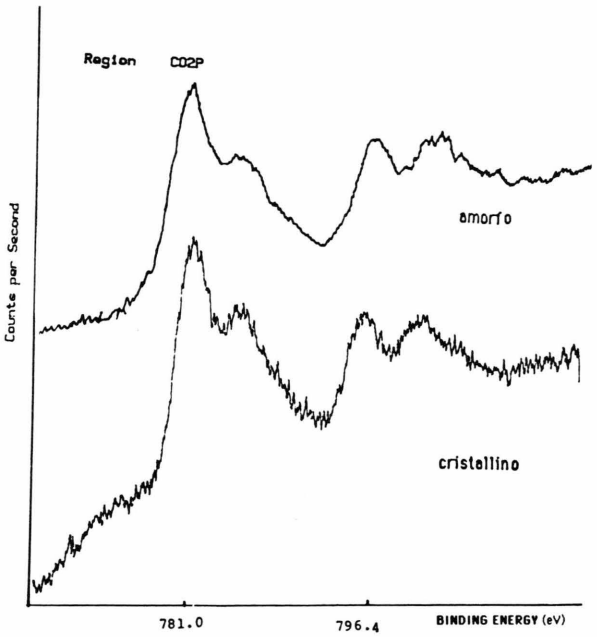

Fig. 4. XPS spectra of Co 2p levels for $Co_2(EDTA) \cdot 6H_2O$, amorphous and crystalline.

Table 3. Core-level binding energies (eV) of N1s and O1s.

Compound	N1s		O1s	
$Na_2(EDTA) \cdot 2H_2O$	401.5 (1.9)	530.9 (1.8)	532.2 (1.8)	533.0 (1.8)
$Ni_2(EDTA) \cdot 6H_2O$ amorphous	399.9 (2.0)	531.5 (2.0)		533.5 (2.0)
$Ni_2(EDTA) \cdot 6H_2O$ crystalline	399.9 (1.9)	531.4 (1.8)		533.4 (1.9)
$Co_2(EDTA) \cdot 6H_2O$ amorphous	400.6 (2.0)	531.2 (1.8)		533.3 (1.8)
$Co_2(EDTA) \cdot 6H_2O$ crystalline	399.9 (2.0)	531.6 (1.8)		533.3 (1.9)

tic nickel complexes by Frost et al. [17] and Matienzo et al. [7].

The shift of 2.2 eV to higher binding energy for the 2p levels may be due to a decrease in the electron density surrounding the cation.

The binding energies (Table 3) of N1s and O1s for $Ni_2(EDTA) \cdot 6H_2O$ are shifted with respect to those observed in $Na_2(EDTA) \cdot 2H_2O$, and this finding confirms that both atoms are involved in the coordination to the nickel cation.

The width of the Ni^{2+} spectrum seems to depend on crystallinity, and it is 2.6 eV for the crystalline compound and 2.9 eV for the amorphous one under instrumental condition with FWHM 1.7 eV for Au 4f 7/2.

Figure 4 shows the Co 2p levels in amorphous and crystalline $Co_2(EDTA)(H_2O)_4 \cdot 2(H_2O)$.

The 2p levels in both complexes are found to be at 781.0 eV and 796.6 eV, respectively (Table 2). There is no relevant change in the spin-orbit splitting ($\Delta = 15.6$ eV). The FWHM of Co 2p 3/2 changes from 3.9 eV in amorphous $Co_2(EDTA)(H_2O)_4 \cdot 2H_2O$ to 3.7 eV in crystalline one.

There is a clear indication of a complex satellite structure which could be deconvolved to distinguish two pairs of satellite lines at about 3.4 eV and 7.2 eV. These findings indicate that the two complexes are both high spin Co^{2+} compounds, and since the separation of the satellite lines from the main peak depends on the coordination number and the covalency of the chemical bond [18–19] it can be concluded that in both cases the cobalt ion has an octahedral coordination. From the N1s and O1s binding energies we can say that both these atoms are involved in the coordination to the cobalt cation.

It has been shown [20] that the 2p peakwidth (FWHM) increases from amorphous to crystalline compounds as we pointed out for this compound.

Conclusions

The objective of this study was to compare the short local structure of amorphous complexes $Ni_2(EDTA)(H_2O)_4 \cdot 2(H_2O)$ and $Co_2(EDTA)(H_2O)_4 \cdot 2(H_2O)$ with the crystalline structure.

LAXS and XPS analyses have clearly shown the great similarity of the short range order of the structures for both complexes.

Acknowledgements

The authors wish to express their grateful appreciation to Prof. Domenico De Filippo for the helpful discussion and the constant encouragement.

Financial support by Ministero degli Affari Esteri (Italian Government) for the fellowships to C. Munoz Roca and J. A. Real Cabezos and financial support by Ministero della Pubblica Istruzione (40%) is gratefully acknowledged.

[1] R. Caminiti, J. Mol. Liquids **1984,** 191.
[2] A. Mosset, J. Galy, E. Coronado, M. Drillon, and D. Beltran, J. Amer. Chem. Soc. **106,** 2864 (1984).
[3] J. J. Del Val, L. Esquivias, P. L. Olano, and F. Sanz, J. Non-cryst. Solids **70,** 211 (1985).
[4] R. Caminiti, G. Johansson, and I. Toth, Acta Chem. Scand. A **40,** 435 (1986).
[5] K. Siegbahn, C. Nordling, A. Fahlman, R. Nordberg, H. Hamrin, J. Hedman, G. Johnson, T. Bergmark, S. K. Karlsson, I. Lindgren, and B. Lindberg, ESCA, Atomic, Molecular and Solid State Structure by means of Electron Spectroscopy. Almquist & Wiksell, Uppsala 1967.
[6] K. Siegbahn, C. Nordling, G. Johnson, J. Hedman, P. Hedan, K. Hamrin, U. Gelius, T. Werme, R. Manne, and Y. Baer, ESCA applied to free molecules, North-Holland, Amsterdam 1969.
[7] L. J. Matienzo, Lo I. Yin, Samuel O. Grim, and W. E. Swartz jr., Inorg. Chem. **12,** 12, 2762 (1973).
[8] C. A. Tolman, W. M. Riggs, W. J. Linn, C. M. King, and R. C. Wendt, Inorg. Chem. **12,** 12, 2770 (1973).
[9] D. C. Frost, C. A. McDowell, and J. S. Woolsey, Mol. Phys. **27,** 1473 (1974).
[10] W. L. Jolly, D. N. Hendrickson, and J. M. Hollander, Inorg. Chem. **8,** 2642 (1969).
[11] A. I. Pozhidaev, N. N. Neronova, T. N. Polynova, M. A. Porai-Koshits, and V. A. Logvinenko, Zhurnal Strukturnoi Khimii **13,** (μ° 2) 344 (1972).
[12] E. F. K. McCandlish, T. K. Michael, J. A. Neal, E. C. Lingafelter, and N. J. Rose Inorg. Chem. **17,** (μ° 6) 1383 (1978).
[13] D. Beltram, E. Escriva and M. Drillon, J. Chem. Soc. Faraday Trans. **2,** 78, 1773 (1982).
[14] R. Caminiti and G. Johansson, Acta Chem. Scan. A **35,** 373, (1981).
[15] Int. Tables for X-Ray Crystallography, Vol. **4,** Kynoch Press, Birmingham 1974.
[16] D. T. Cromer, J. Chem. Phys. **50,** 4857 (1969).
[17] D. C. Frost, C. A. McDowell, and I. S. Woolsey, Mol. Phys. **27,** 1473 (1974).
[18] S. Larsson, Chem. Phys. Lett. **40,** 3, 362 (1976).
[19] C. Battistoni, L. Gastaldi, G. Mattogno, M. G. Simeone, and S. Viticoli, Solid State Comm **61,** 1, 43 (1987).
[20] K. Asami, K. Hashimoto, and S. Shimodaira, Corr. Sci. **16,** 35 (1976).